Bio-Energy with CCS (BECCS) performance evaluation: efficiency enhancement and emissions reduction

Mai Bui[a,b], Mathilde Fajardy[a,b], Niall Mac Dowell[a,b,*]

[a] *Centre for Process Systems Engineering, Imperial College London, South Kensington, London SW7 2AZ UK*

[b] *Centre for Environmental Policy, Imperial College London, South Kensington, London SW7 1NA UK*

Abstract

In this study we evaluate the feasibility of the recovery of waste heat from the power plant boiler system of a pulverised fuel power plant with amine-based CO_2 capture. This recovered heat can, as a function of fuel type and solvent selection, provide up to 100% of the heat required for solvent regeneration, thus obviating the need for withdrawing steam from the power plant steam cycle and significantly reducing the efficiency penalty imposed upon the power plant by the CO_2 capture process. In studying the thermochemistry of the combustion process, it was observed that co-firing with low moisture biomass achieved higher adiabatic flame temperatures (AFT) than coal alone. The formation and emission of SO_X reduced as biomass co-firing proportion increased, whereas NO_X emissions were observed to be a function of AFT. The power generation efficiency of a 500 MW 50% co-firing BECCS system increased from $31\%_{HHV}$ with a conventional MEA solvent, to $34\%_{HHV}$ with a high performance capture solvent. The heat recovery approach described in this paper enabled a further efficiency increase up to $38\%_{HHV}$ with the high performant solvent. Such a system was found to remove 0.83 Mt_{CO_2} from the atmosphere per year at 90% capacity factor.

Keywords: Bio-energy, Carbon Capture and Storage (CCS), BECCS, Greenhouse gas removal (GGR), Negative emissions technologies (NETs)

*Corresponding author

Email address: niall@imperial.ac.uk (Niall Mac Dowell)

1. Introduction

Carbon capture and sequestration (CCS) technologies are well accepted as being vital for the mitigation of climate change [1]. There is growing interest in developing long-term CO_2 mitigation strategies that have the potential for deep reductions in atmospheric CO_2 concentrations. CCS with so-called negative emissions technologies (NETs) or greenhouse gas removal (GGR) technologies are expected to play an essential role in limiting global warming below 2°C, as advised by IPCC [2] and in meeting the 1.5°C target proposed by COP21 [3]. "Negative emissions" technology that combines biomass-derived energy and CO_2 sequestration was first introduced by Williams (1996) [4] for hydrogen fuel production and Herzog (1996) [5] for electricity generation. Biomass grown and harvested sustainably is considered an appropriate substitute for fossil fuels [6, 7]; during growth, there is a net transfer of atmospheric CO_2 into biomass, and the conversion of the biomass to produce electrical energy and the capture and geological storage of the arising CO_2 enables the permanent removal of that CO_2 from the atmosphere [8, 9]. This is referred to as bio-energy with carbon capture and sequestration, or BECCS [10, 11, 12, 13][1], and can achieve an overall negative CO_2 balance when carefully deployed [14, 15, 16, 17, 8, 18, 19, 20, 10]. The IPCC highlighted BECCS as an important mitigation option in the fifth assessment report [2], and it was the most widely selected negative emissions technology by integrated assessment models to meet temperature targets [9].

In addition to reducing CO_2 emissions, biomass co-combustion has been shown to reduce NO_X, SO_X and particulate emissions [21]. Full-scale studies demonstrate that high proportions of biomass co-firing is possible without any effect on boiler or combustion efficiency, provided modern burner technology is used [22]. Dedicated biomass combustion at the utility scale is possible with, for instance, the Drax Power Station operating two of its 660 MW generating units with a 100% biomass fuel [23]. The conversion of these units from coal

[1] Originally termed BECS by Kraxner *et al.* (2003) [8]

to biomass is reported to have cost £700M, which covered all capital required for the storage, handling and conversion of the biomass [24]. On the other hand, biomass-dedicated power plants are typically one-tenth the size (1 to 100 MW) of conventional coal-fired plants, due to limited biomass availability and high cost of transportation [25, 26]. Fuel availability is region specific, as there will be variation in feedstock properties, land/water availability, crop yields, transportation costs and other parameters. However, biomass supply chains in the UK have yet to fully develop. Consequently, large-scale plants such as Drax must import wood pellets to meet fuel requirements, 58% from the US, 21% from Canada, and 7.5% from Latvia [27].

Biomass tends to have a lower heating value and often higher moisture content compared to high quality coal (shown by table A1). Therefore, biomass co-combustion tends to reduce power plant output relative to dedicated coal combustion [28], for a constant fuel combustion rate. The addition of CO_2 capture technology will impose a further energy penalty, appreciably reducing electricity output per unit of primary fuel utilised [29]. The size of a biomass power plant needs to be large enough to exploit economy of scale, however, size is limited by biomass availability and cost [26]. When the capacity of an electricity generation plant is doubled, capital cost increases approximately 62%. Larger power plants are more thermally efficient than small-scale plants. For instance, a 200 MW power plant converts 30–39% of the thermal energy into electricity, whereas a 25 MW plant converts 20–25% into electricity [30]. Subsequently, the cost of generating electricity is higher for small-scale power plants [31]. Ultimately, the higher thermal efficiency and lower cost of electricity generation make larger facilities more profitable than small-scale plants, thus outweighing the higher construction costs [30].

2. Enhancement of BECCS performance

In comparison to other energy systems, BECCS is a promising candidate for negative emissions (as shown by figure 1). In the near to medium term, most, if

not all, BECCS power plants will continue to compete in liberalised electricity markets. Thus, efficiency improvements will serve to reduce the marginal cost of electricity generation, allowing the facility to operate at a higher load factor [32, 33]. Therefore, further improvements to its performance will encourage large scale deployment of the technology.

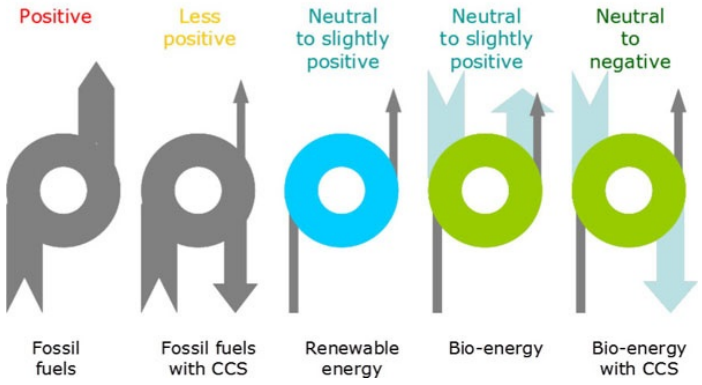

Figure 1: Net carbon balance for various energy conversion systems [34].

In conventional post-combustion capture technology, heat is supplied to the solvent regeneration process in the form of saturated steam. This reboiler heat duty (HD in $\mathrm{MJ/t_{CO_2}}$) is the summation of three contributions: (i) the sensible heat to raise the solvent from absorber to desorber temperature; (ii) the heat of evaporation to produce the steam supplied to the reboiler; and (iii) the heat of absorption, *i.e.* the heat necessary to desorb the CO_2 from the solution [35]:

$$HD = \frac{Cp \times (T_{\mathrm{R}} - T_{\mathrm{feed}})}{\Delta\alpha} \frac{M_{\mathrm{sol}}}{M_{\mathrm{CO_2}}} \frac{1}{x_{\mathrm{solv}}} + \Delta h_{\mathrm{vap,H_2O}} \frac{p_{\mathrm{H_2O}}}{p_{\mathrm{CO_2}}} \frac{1}{M_{\mathrm{CO_2}}} + \frac{\Delta h_{\mathrm{abs,CO_2}}}{MW_{\mathrm{CO_2}}} \quad (1)$$

where $\mathrm{C_p}$ is the specific heat of the solution, $\mathrm{T_R}$ and $\mathrm{T_{feed}}$ are the temperatures at the reboiler and desorber inlet, respectively, $\Delta\alpha$ is the difference in CO_2 loading between the absorber outlet (rich) and inlet (lean), x_{solv} is the solvent mole fraction in the solution, $\mathrm{\Delta h_{vap,H_2O}}$ is water latent heat of evaporation, $\mathrm{p_{H_2O}}$ and $\mathrm{p_{CO_2}}$ are the vapor and CO_2 partial pressures in the gas phase at the

desorber top, $\Delta h_{abs,CO_2}$ is the heat of absorption of solvent, lastly, MW_{CO_2} and MW_{sol} are the molecular weights of CO_2 and the solution.

This solvent regeneration process requires low grade thermal energy, on the order of 150°C, typically provided by the condensation of steam at ∼3 bar [36, 29]. The main steam supply for CO_2 capture is extracted from the steam cycle of the power plant, which incurs an efficiency penalty on the system [37, 38]. To minimise the efficiency penalty associated with CO_2 capture, several options for extracting steam from the power plant steam cycle have been proposed: steam extraction from the cross-over pipe between the intermediate pressure (IP) and the low pressure (LP) steam turbines [39, 40, 41, 42, 43], steam cycle retrofits designed for optimised integration with CO_2 capture [36, 44], and steam extraction from an appropriate point within the LP turbine [45]. Further improvements to power plant energy efficiency can be achieved through waste heat recovery. Pfaff *et al.* (2010) used waste heat from the CO_2 capture plant to improve the efficiency of the power station. Heat recovered from the stripper overhead condenser and the CO_2 compressor intercoolers were utilised for pre-heating of the steam cycle condensate and combustion air [46]. Another energy source is flue gas heat recovery, which can be used to improve power plant efficiency through fuel drying [47] or applied in a low pressure economiser to heat the condensate in the steam cycle [48, 49, 50, 51]. Alternatively, the heat recovered from flue gas can provide energy for solvent regeneration in CO_2 capture [52, 53], where the measured flue gas temperature at the economiser outlet is ∼345°C [54].

All of these studies on efficiency improvements have focussed on applications in fossil fuel-fired power plants. However, there is relatively little work on efficiency improvement in biomass-fired plants. In a 500 MW supercritical power station co-firing biomass and coal, the temperature of the exhaust gas leaving the boiler can reach 370°C [55]. Therefore, the additional recovery of relatively low-grade heat from the boiler system has the potential to improve the power generation efficiency of a BECCS power plant, albeit at the cost of the additional capital associated with the heat recovery system. Importantly,

the moisture content of biomass can vary significantly; as table A1 demonstrates it varies between 5–60 wt%. As moisture content increases, lower heating value (LHV) decreases due to reduced content of combustible matter per kilogram of biomass [56], which in turn decreases net efficiency of the power plant [55]. However, increased moisture content in the fuel enhances heat transfer properties of the flue gas, thereby improving heat recovery [57].

The quality of biomass has an impact on the system efficiency and heat recovery potential of the flue gas. Specifically, suppose we have the option of a high quality (low moisture, high heating value and likely higher cost) or a low quality (high moisture, low heating value and likely lower cost) fuel. In order to produce a constant amount of power, less of the high quality fuel will be required, leading to less recoverable heat in the boiler system. In the case of a low quality fuel, the contrary is true. This is simply another way of saying that high quality fuels tend to result in improved thermal efficiency, and reduced stack losses than low quality fuels. Hence, the amount of recoverable heat within the boiler will depend on fuel quality. This study comprehensively evaluates the potential use of this recovered heat for solvent regeneration in BECCS systems. The remainder of the paper is structured as follows: we first present engineering and thermodynamic models of the BECCS system. The effect of biomass quality and co-firing proportion on combustion performance was then studied in terms of their impact on adiabatic flame temperature, NO_X emissions and SO_X emissions. The impact of biomass co-firing, heat recovery and solvent selection on system efficiency and carbon intensity is also evaluated. Lastly, the paper concludes with some perspectives for future work in this area.

3. Model development

3.1. Overall algorithm

This section presents the thermodynamic modelling approach used in this work, with a graphical overview of the algorithm presented in figure 2, which show the following steps (denoted by the circled numbers):

1. Selection of the fuels and solvent.
2. Calculation of the fuel flow rate and net power output in the Integrated Environment Controlled Model (IECM, [58]) for different biomass co-firing proportions, based on a 500 MW ultra-supercritical power plant.
3. Model the co-combustion of biomass with coal in FactSage to determine the exhaust gas composition, flow rate, thermodynamic properties and adiabatic flame temperature (AFT).
4. Heat recovery calculations to determine the influence of exhaust gas heat recovery on overall power plant efficiency and carbon intensity.

3.2. Power plant and post-combustion capture model

3.2.1. Fuel selection

Different coal and biomass types were selected from the literature in order to have a representative range of fuel composition and quality scenarios, with respect to moisture content, sulphur content and ash content. Wood biomass and herbaceous biomass have very different properties as seen in Table A1. Thus, a biomass was chosen to represent each of these fuel categories. Dried (5% moisture) and raw (50% moisture) clean wood chip were selected as the low ash content biomass; and dried (5% moisture) and raw (16% moisture) wheat straw were selected as the high ash content biomass. Two bituminous coals with medium (0.9%) and high sulphur content (2.5 %), and relatively similar moisture content ($\approx$ 10%) were selected. Tables 1 and 2 summarise the higher heating value (HHV) and composition of the biomass and coals; the ash composition is in table A2. The blended fuel composition was then determined for these fuels at different biomass-coal co-firing proportions.

3.2.2. Solvent selection

The characteristics of the CO_2 capture solvents used in calculations are summarised in table 3. Monoethanolamine (MEA) was used as the base case with a reboiler heat duty of 3600 MJ.$t_{CO_2}{}^{-1}$ (average calculated by IECM, [58]), and a reboiler temperature of 120°C. The second capture system scenario

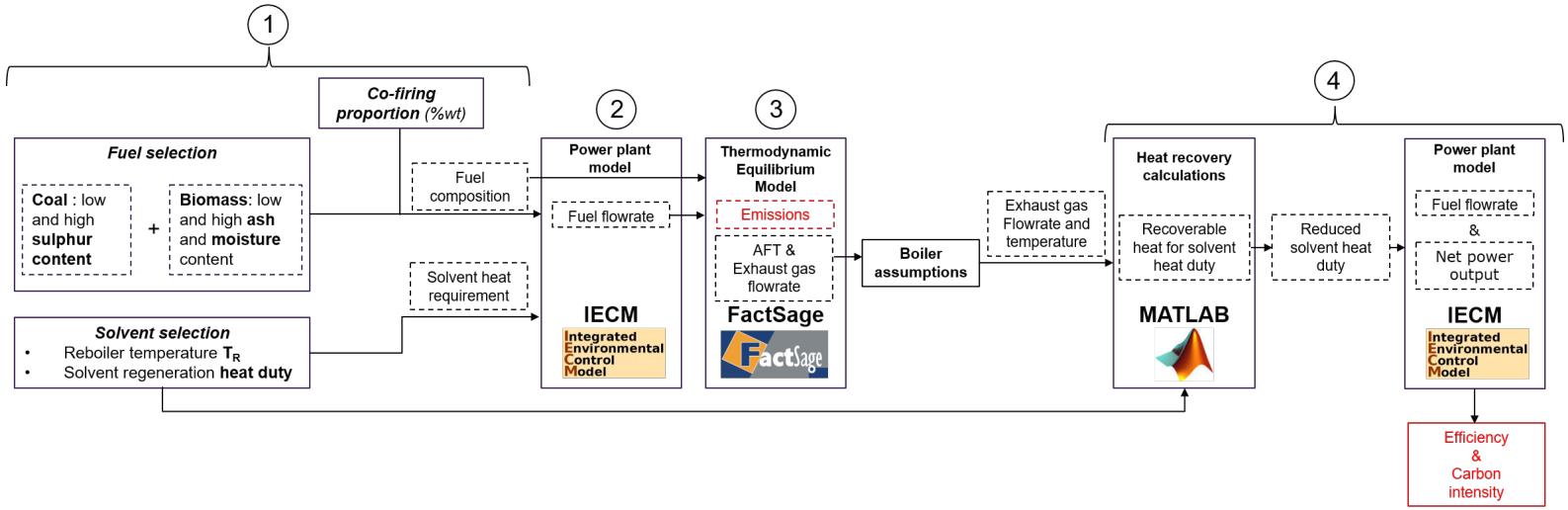

Figure 2: Model algorithm used to evaluate the effect of flue gas heat recovery on process performance.

Table 1: Biomass dry basis composition.

Composition	Clean wood chips	Wheat straw
HHV ($MJ.kg^{-1}$ dry)	19.16	19.22
C (dry wt%)	50	48.7
H (dry wt%)	5.4	5.7
O (dry wt%)	42.2	39.1
Cl (dry wt%)	0.02	0.32
S (dry wt%)	0.05	0.1
N (dry wt%)	0.3	0.6
Ash (dry wt%)	2.0	5.5
References	[59]	[60, 61, 62, 63]

Table 2: Coal wet basis composition.

Composition	High sulphur coal	Medium sulphur coal
HHV ($MJ.kg^{-1}$ dry)	27.14	27.06
C (wt%)	63.75	64.6
H (wt%)	4.5	4.38
O (wt%)	6.88	7.02
Cl (wt%)	0.29	0.023
S (wt%)	2.51	0.86
N (wt%)	1.25	1.41
Ash (wt%)	9.7	12.2
Moisture (wt%)	11.12	9.5
References	[58]	[59]

used parameters representative of Cansolv; a commercial solvent with a reboiler heat duty of 2300 $MJ.t_{CO_2}{}^{-1}$ and a reboiler temperature of 120°C [64, 65]. Ye *et al.* (2015) achieved an overall heat duty reduction of 30% with biphasic solvent compared with conventional MEA systems [66]. Biphasic (or dual-phase) systems can involve liquid-solid separation (*e.g.* aqueous ammonia) or liquid-liquid separation, and have lower energy requirements in comparison to single-

phase absorption systems. Liquid-solid systems have the advantages of increased CO_2 absorption capacity and improved energy efficiency in the stripper [67]. In liquid-liquid systems, energy consumption reduces due to: (i) the decrease of the liquid amount sent to the stripper, and (ii) a reduction of the desorption temperature (characteristic of biphasic solvents) [68]. As suggested in Ye et al. (2015) temperatures of between 80–120°C were chosen for the reboiler operating temperature. As MEA heat duty reported in IECM is quite conservative, and substantially lower values have been reported in the literature, therefore 2900 $MJ.t_{CO_2}{}^{-1}$ [69] was considered to be representative of the limits of what could be achieved with MEA solvent. Thus, using 2,900 $MJ.t_{CO_2}{}^{-1}$ as a baseline, an energy of regeneration of 2,000 $MJ.t_{CO_2}{}^{-1}$ at 80°C was judged to be on the limit of what is achievable with state-of-the-art solvents [70, 71, 72].

Table 3: Solvent characteristics.

Solvent	Heat duty ($MJ.t_{CO_2}{}^{-1}$)	Reboiler temperature (°C)
MEA	3600	120
Cansolv	2300	120
"New solvent"	2000	80

3.2.3. Power plant model

An ultra-supercritical 500 MW coal-fired power plant with a 90% post-combustion capture rate and a cooling tower was modelled in IECM. In this configuration and for a given fuel composition, IECM enables the calculation of the fuel flow rate, F_F (in t/hr), necessary to meet the 500 MW capacity and the power plant net power output, NPO, in MW.

In this study, the technical and environmental performance of the power plant is assessed with respect to two metrics: efficiency and carbon intensity. Carbon intensity is defined at the power plant algebraic emissions per MW produced. Based on the fuel higher heating value (HHV, in MWh/t), the net power generation efficiency η (in % HHV) can then be calculated using the

following formula:

$$\eta = \frac{NPO}{F_{\mathrm{F}} \times HHV} \tag{2}$$

The carbon negativity of BECCS is contingent on 90% of the emitted CO_2 being captured, of which a certain fraction (the co-firing proportion, Cf) has been captured from the atmosphere by the biomass. Based on the fuel carbon content, C_F, the biomass carbon content, C_B, and the co-firing proportion, the overall carbon intensity CI (in kg_{CO_2}/MWh) was calculated with the following equation:

$$CI = \frac{F_{\mathrm{F}}((1 - R_{\mathrm{CCS}}) \times C_F - Cf \times C_B) \times \frac{MW_{\mathrm{CO_2}}}{MW_{\mathrm{C}}}}{NPO} \times 1000 \tag{3}$$

where $\mathrm{MW_{CO_2}}$ and $\mathrm{MW_C}$ are the molecular weights of CO_2 and carbon, respectively.

3.3. Chemical equilibrium model of biomass co-combustion with coal

A thermo-chemical analysis of coal co-combustion with biomass was conducted using the software FactSage 7.0, which has access to thermodynamic data from the FACT and SGTE[2] databases. Based on the specified temperatures, pressure and composition of fuel and air, FactSage calculates the species formed once chemical equilibrium is reached after complete or partial reaction [73, 74]. FactSage is capable of handling a wide range of biomass combustion and condensation products[3] [75].

Table 4 summarises the fuel blending scenarios of coal and biomass that were modelled in FactSage. For each scenario, biomass co-firing proportion was increased from 0% to 50% in increments of 5%. IECM provided data for fuel

[2]The FACT databases were developed as part of the FACT Database Consortium Project, whereas SGTE databases were prepared by the international Scientific Group Thermodata Europe (SGTE) consortium [73, 74].

[3]Condensation products form when volatilised solids are cooled to form droplets, which may deposit on a surface or remain suspended in the gas stream.

firing flow rates based on the blended fuel composition in a 500 MW ultra-supercritical power plant. The fuel flow rates in tonnes per hour was used as the mass basis in the equilibrium calculations.

Table 4: Biomass and coal co-firing scenarios modelled in FactSage.

Scenario	Fuel blend
A	Medium sulphur coal and wheat straw of 5% moisture
B	Medium sulphur coal and wheat straw of 16% moisture
C	Medium sulphur coal and wood chip of 5% moisture
D	Medium sulphur coal and wood chip of 50% moisture
E	High sulphur coal and wheat straw of 5% moisture
F	High sulphur coal and wheat straw of 16% moisture
G	High sulphur coal and wood chip of 5% moisture
H	High sulphur coal and wood chip of 50% moisture

Supplying the optimal amount of air is critical for efficient combustion, to minimise thermal losses and to ensure complete combustion. To achieve complete combustion, the excess air coefficient (λ) typically ranges from 1.1–1.8 for large scale applications and 1.5–2.0 for small scale systems[4], depending on the combustion technology [76]. In this study, $\lambda = 1.3$ was used for all combustion simulations in FactSage, as this ensured complete combustion and maintained an O_2 concentration of ∼5–6% in the flue gas, in line with common industrial practice.

FactSage was used to calculate the adiabatic flame temperature (AFT) of each fuel blend of biomass and coal. Then co-combustion of each fuel blend was simulated from 200°C to the AFT. Subsequently, the multi-phase flue gas mixture was cooled from the AFT to 370°C, representing an energy transfer to

[4]Small-scale combustion systems are used for domestic applications (*e.g.* heating boilers, wood stoves) with a nominal boiler capacity of ∼100 kW_{th}. The large-scale combustion applications are the range of MW_{th} or greater, which include district heating, electricity generation, process heating and combined heat and power systems [76].

the power plant steam cycle. The analysis of SO_X and NO_X emissions were analysed at 370°C (flue gas temperature of the boiler exit predicted by IECM [55]). Note, however, the temperature of the flue gas at the boiler exit is a function of the AFT, which in turn, varies with different fuels and co-firing proportion. Typically, the energy transferred to the steam cycle should be held constant. Thus, increases in AFT represent the potential for greater heat recovery. The AFT for different fuel blends was an important consideration in the heat recovery analysis as it quantified the degree of variation in flue gas temperature at the boiler exit.

The objective of this analysis was to study the influence of biomass co-firing proportion on: (i) AFT, (ii) SO_X and NO_X emissions, and (iii) properties of the exhaust gas. The exhaust gas properties (flow rate and specific heat capacity) and AFT were required for the heat recovery analysis in the next section. FactSage assumes equilibrium thermochemistry, and whilst it is recognised that this is not representative of all conditions within the boiler, it does provide insight into the limits of species formation [77, 78] and is reliable for the calculation of flame temperatures.

3.4. Heat recovery calculations

A heat recovery model (figure 3) was designed in MATLAB to calculate the amount of recoverable heat from the boiler system and the exit flue gas temperature for the different co-firing proportion and solvent scenarios.

In a first instance, the reboiler heat duty (HD in $MJ.t_{CO_2}{}^{-1}$) of the solvent scenario, and the amount of CO_2 (F_{CO_2} in $t_{CO_2}.hr^{-1}$) to be processed by the post-combustion capture system for the specific co-firing proportion, are used to calculate the overall heat rate required for the reboiler Q_R:

$$Q_R = HD \times F_{CO_2} \tag{4}$$

For the given reboiler temperature, T_R, in order to ensure efficient heat transfer, it was assumed that the reboiler saturated steam inlet temperature, T_o, was 20K greater than the reboiler temperature and that the reboiler sub-saturated

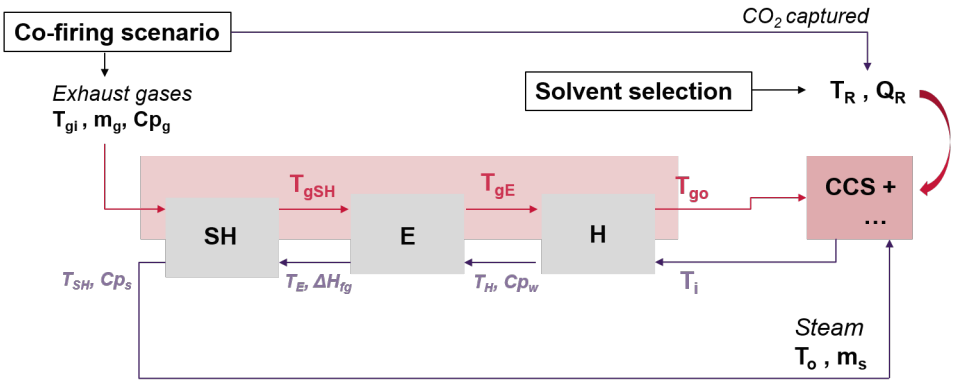

Figure 3: Illustration of the heat recovery model (H=Heater, E=Evaporator, SH=Super heater).

water outlet temperature, T_i, would be 5K below the inlet temperature, *i.e.*, assuming a minimal amount of condensate sub-cooling:

$$T_o = T_R + 20 \tag{5}$$

$$T_i = T_o - 5 \tag{6}$$

The pressure P_o of the reboiler steam inlet is assumed to be the saturation pressure at T_o. The steam flowrate m_s (in t.hr^{-1}) can then be determined:

$$m_s = \frac{Q_R}{\Delta H_g(T_o)} \tag{7}$$

where ΔH_g is the enthalpy of saturated steam at T_o and P_o.

The aim here is to incorporate an additional low pressure steam loop within the boiler system, comprising of a heater, an evaporator and a super-heater [79]. The exit temperature of the heater, T_H, is the saturated temperature at P_o, T_o, the evaporator is isothermal, and the superheater was assumed to heat the steam by 5°C to compensate for heat losses up to the reboiler, in other words, the aim is to deliver saturated steam to the reboiler. Sub-saturated water, saturated steam and super-heated steam thermodynamic properties were taken

from steam tables [80], [81]. For the three units, the following thermodynamic relations were used:

$$Q_H = m_s \times Cp_w \times (T_H - T_i) \tag{8}$$

$$Q_E = m_s \times \Delta H_{fg}(T_E) \tag{9}$$

$$Q_{SH} = m_s \times Cp_s \times (T_{SH} - T_E) \tag{10}$$

The exhaust gas flow rate, m_g, temperature, T_{gi} and heat capacity, Cp_g, are known for each scenario, and the amount of heat transferred gives the exhaust gas temperature profile along the heat exchanger:

$$T_{gSH} = T_{gi} - \frac{Q_{SH}}{Cp_g \times m_g} \tag{11}$$

$$T_{gE} = T_{gSH} - \frac{Q_E}{Cp_g \times m_g} \tag{12}$$

$$T_{go} = T_{gE} - \frac{Q_H}{Cp_g \times m_g} \tag{13}$$

The heat exchanger area, A, is the sum of area for the three sections, determined with the log mean temperature (ΔTm) model [82] and overall heat transfer coefficients from literature (provided in table 5 for completeness):

$$A_H = \frac{Q_H}{U_H \times \Delta Tm_H} \tag{14}$$

$$A_E = \frac{Q_E}{U_E \times \Delta Tm_E} \tag{15}$$

$$A_{SH} = \frac{Q_{SH}}{U_{SH} \times \Delta Tm_{SH}} \tag{16}$$

$$A = A_H + A_E + A_{SH} \tag{17}$$

Table 5: Overall heat transfer coefficients

Overall transfer coefficient ($W.m^{-2}$)	Value	Source
U_H	50	Luyben et al, 2014 [79]
U_E	280	Luyben et al, 2014 [79]
U_{SH}	170	Perry & Green, 2008 [83]

For each solvent and co-firing proportion, the fraction of reboiler heat duty that can be supplied by energy from heat recovery was calculated. Finally, the reduced heat duty value was then implemented in IECM to determine the new system efficiency and carbon intensity.

4. Results and Discussion

4.1. Co-combustion of biomass with coal

4.1.1. Adiabatic flame temperature (AFT)

Adiabatic flame temperature is calculated based on the sensible enthalpy, enthalpy of formation and temperature-dependent specific heat capacity data for the chemical species in the fuel [84]. The calculated AFT changes with different fuel compositions (*i.e.* different reactant stoichiometry or chemical species) or initial temperature. Figure 4 illustrates the differences in calculated AFT for various biomass and coal blends. The AFT generally increased with higher biomass co-firing percentage. The FactSage modelling revealed that AFT continues to increase linearly as the biomass co-firing proportion is increased up to 100%. Although higher heating value (HHV) of the blended fuel reduced as biomass co-firing % increased, the fuel firing rate increased to meet the specified capacity of the power plant (500 MW). This effect was replicated in FactSage by increasing the mass basis in accordance to the fuel firing rates predicted by IECM. The published AFT range for different biomass (dry basis) fuels is 1730–2430°C [85], whereas coal varies between 1900–2230°C [86]. Therefore, the values of AFT calculated by FactSage for biomass and coal co-combustion (2182–2324°C) is within the ranges reported in literature.

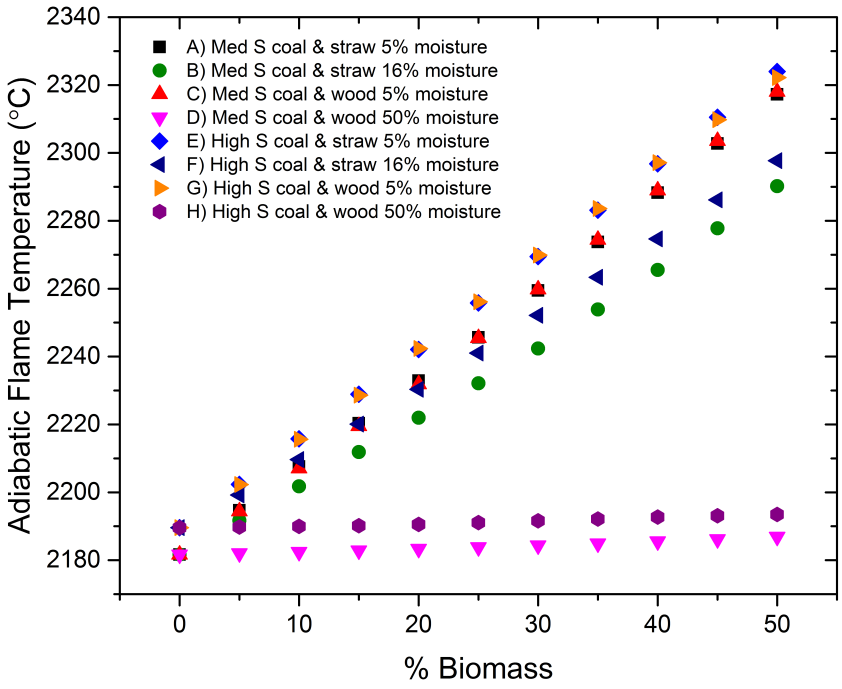

Figure 4: Adiabatic flame temperature for the combustion of various biomass and coal blends at different biomass co-firing % and $\lambda = 1.3$.

The moisture of the fuel limits the combustion performance due to the: (i) reduction in heating value, and (ii) evaporation of water, which is endothermic and hinders the exothermic combustion reaction. To ensure the combustion of biomass is self-sustaining, the limit for maximum moisture content is ~65% wet basis. The ash content also reduce heating value of the fuel as it does not contribute to the release of heat during combustion [85]. As demonstrated by Sami *et al.* (2001), increased composition of ash and moisture results in decreased AFT. Additionally, AFT can reduce with increased amount of stoichiometric

air[5] [86]. To prevent flame instability in boilers and furnaces, the temperature needs to remain above 1600 K [86]. Thus, understanding the effect of fuel content and combustion conditions on AFT is essential.

Variations in composition for different fuel types and blends influence the AFT, and thus can impact the boiler performance. When comparing AFT of 0% and 50% biomass for the different co-firing scenarios in table A3, biomass moisture content had a significant effect on the degree of increase in AFT. Increasing the co-firing proportion of high 50% moisture wood chip from 0% to 50% with medium sulphur and high sulphur coal increased AFT by 5.26°C and 3.91°C, respectively. Although moisture content was high, AFT increased slightly due to the reduction in ash content as biomass % increased[6]. In comparison, co-firing coal with moderate 16% moisture straw resulted an increase 108°C in AFT. The greatest increase in AFT was achieved with the co-combustion of low 5% moisture biomass with coal, which led to a major increase in AFT of 136°C (scenarios A and C of medium S coal and 5% moisture wood/straw). The moisture content of the medium sulphur coal and high sulphur coal was 9.5 wt% and 11.1 wt%, respectively. In other words, co-firing with a biomass of low moisture content enhanced the combustion performance of a low rank coal.

The co-combustion of the same biomass type with high sulphur coal led to higher AFT than co-combustion with medium sulphur coal. As indicated by Sami *et al.* (2001), the higher ash content in medium sulphur coal compared to high sulphur coal (table 2) would result in lower AFT values. Additionally, the ash content of wood chip and wheat straw was significantly lower than the two coals. Hence, increased biomass co-firing percentage reduced the overall ash content of the fuel blend, leading to higher adiabatic flame temperatures.

[5]The presence of excessive amounts of air cools down the combustion process, leading to thermal losses and incomplete combustion [76]

[6]For the medium sulphur coal case, when the co-firing proportion of 50% moisture wood chip was increased from 0 to 50%, the overall ash content reduced from 12.2 to 6.6 wt% wet basis. In the case of high sulphur coal, ash content reduced from 9.7 to 5.4 wt% wet basis

4.1.2. SO_X and NO_X emissions

The emissions of SO_X are represented as concentration in the exhaust flue gas at 370°C in units of parts per million weight basis (ppm). Figures 5, 6 and 7 demonstrate that co-combustion of biomass with coal significantly reduced SO_X emissions, which concurs with previous research [87, 61, 88, 86, 89, 90, 91]. Although the regions of highest AFT correlate with the lowest SO_X emissions, it is unlikely that these two parameters are related. The main reasons for the decrease in SO_2 emissions are: (i) reduction in sulphur content of the fuel, (ii) presence of specific ash components that can absorb SO_2 [61].

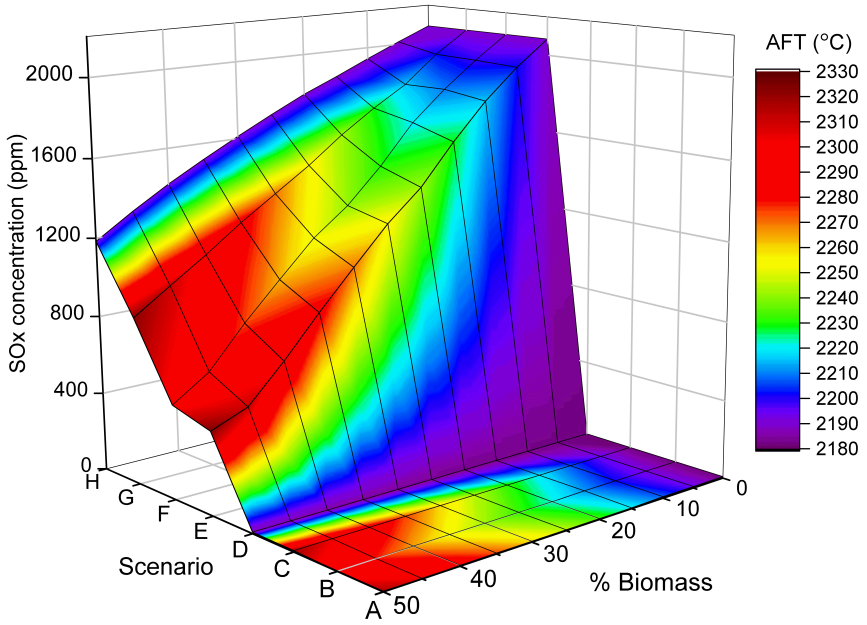

Figure 5: The influence of biomass co-firing % on SO_X emissions in relation to AFT. Letters on the Scenario axis correspond to fuel blends in table 4.

Experimental studies suggest that SO_X emissions decrease linearly with increased biomass co-firing % [87, 61, 88, 90]. This linear trend is apparent for biomass co-combustion with high sulphur coal. As figure 6 illustrates, the de-

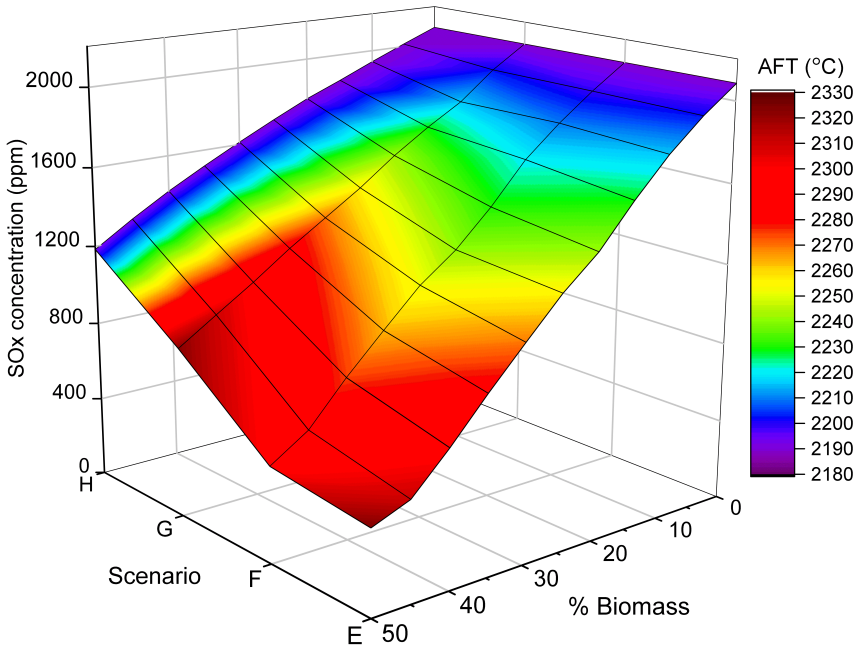

Figure 6: The influence of biomass co-firing % on SO_X emissions for high sulphur coal blends in relation to AFT. Letters on the Scenario axis correspond to fuel blends listed in table 4.

crease in SO_X emissions is proportional to the amount of biomass co-fired with high sulphur coal. The major reason for this decrease in SO_X emissions is due to the significantly lower sulphur content of wood chip and wheat straw compared to coal.

In contrast, there is a non-linear decrease of SO_X emissions during biomass co-firing with medium sulphur coal (figure 7), and scenario D has constant SO_X emissions. The non-linear behaviour may be due to the shifting of equilibrium reactions that are concentration driven. The formation of SO_X involves a number of mechanisms. During combustion, almost all of the fuel sulphur is oxidised to gaseous compounds (*e.g.* SO_2 and SO_3). The formation of SO_2 is thermodynamically favoured at high temperature (>1000°C), thus SO_2 is the principal SO_X [92]. As temperature decreases, the equilibrium shifts towards the forma-

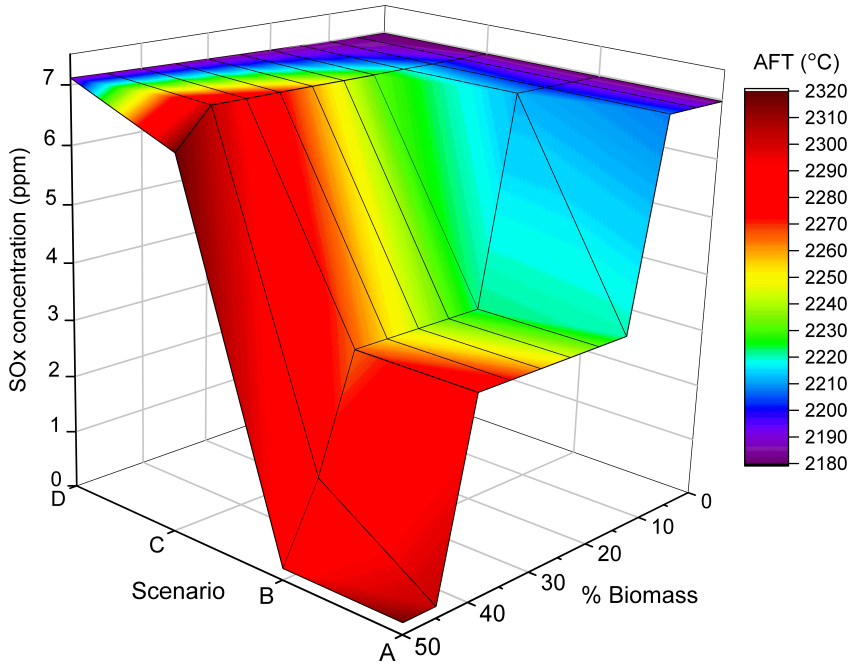

Figure 7: The influence of biomass co-firing % on SO_X emissions for medium sulphur coal blends in relation to AFT. Letters on the Scenario axis correspond to fuel blends in table 4.

tion of SO_3. However, the formation of SO_3 is very slow and typically, only 0.1–1% SO_2 is converted to SO_3 [92, 93, 94]. The presence of iron oxide can catalyse the formation of SO_3 from SO_2 and O_2 [95, 96, 97]. Therefore, the production of SO_3 depends on iron oxide content in the ash and O_2 concentration in the gas stream. The alkali oxides in ash (*e.g.*, CaO, MgO) favour the capture of SO_3 over SO_2. Subsequently, catalytic conversion of SO_2 to SO_3 by iron oxide enhances SO_X removal by ash, thereby reducing emissions [95, 94, 93, 96].

Although the sulphur content of straw (0.1 wt%) is slightly higher than wood (0.05 wt%), co-firing coal with straw achieved lower SO_X emissions compared to wood (figures 6 and 7). This effect is likely due to the ash content of wheat straw (5.5 dry wt%) being greater than wood chip (2 dry wt%). The species distribution in FactSage of the exhaust gas at 370°C revealed that sulphur re-

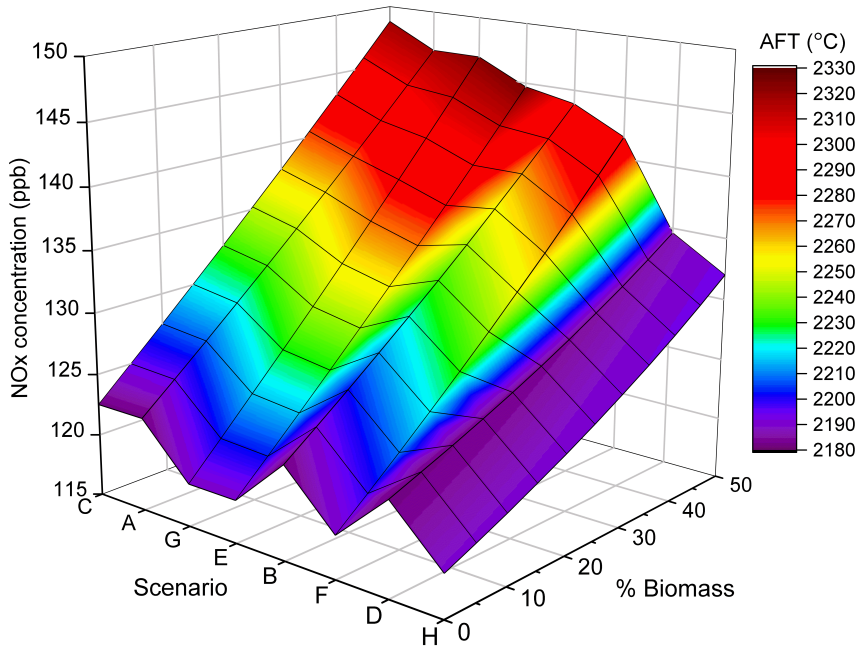

Figure 8: The influence of biomass co-firing % on NO_X emissions (flue gas 370°C) in relation to AFT. Letters on the Scenario axis correspond to fuel blends in table 4.

acted with a number of ash components (Al_2O_3, Fe_2O_3, CaO, MgO, Na_2O, K_2O and MnO_2) to form solid compounds. Although the main ash components reported to have the ability to reduce SO_X are the alkali metal oxides CaO, MgO [61, 95, 98, 93, 94], Na_2O and K_2O [99, 100, 101, 92, 102], it is possible other metal oxides could have a role in SO_X reduction, and may depend on whether equilibrium conditions are satisfied. This analysis highlights the importance of considering ash alkali oxide interactions with sulphur, as they have an essential role in the formation of SO_X.

The concentration of NO_X emissions in the exhaust flue gas (at 370°C) is in units of parts per billion weight basis (ppb), which is significantly lower than SO_X emissions by several orders of magnitude. Although fuel nitrogen content decreased, figure 8 indicates NO_X emissions increased with higher biomass

co-firing proportion. Many experimental studies suggest that NO_X emissions reduce as biomass co-firing % is increased [61, 88, 87, 103, 90, 49] due to decreased fuel nitrogen [104, 105]. However, some report that despite co-firing coal with significant proportions of biomass, NO_X emissions increased [91, 106] or remain unchanged [107] compared to coal only combustion. Hence, it was proposed that NO_X emissions are largely dependent on combustion engineering and operating conditions [61, 88, 103, 91]. The emissions of NO_X tend to reduce at lower temperatures, or conversely, NO_X emission would increase with high temperature combustion [108, 98]. Due to the greater adiabatic flame temperatures with higher biomass co-firing rates, NO_X emissions increased proportionally (figure 8).

The NO_X concentrations at 0% biomass co-firing in figure 8 are for combustion of coal alone. Scenarios A, B, C, D correspond to medium sulphur coal, which have higher nitrogen content compared to the high sulphur coal scenarios (E, F, G, H). During the combustion of coal alone, the medium sulphur coal generates higher NO_X emissions compared to the high sulphur coal, which demonstrates that fuel N-content has a significant role in NO_X formation, which concurs with coal combustion experiments [109]. However, the conversion ratio to NO_X species depends on the degree of nitrogen volatilisation and how much nitrogen remains in the char [110, 111, 112], which vary depending on the combustion conditions (*e.g.* burner aerodynamics, residence time) [110, 113]. A coal combustion study by Hu *et al.* (2000) demonstrates that temperature and the presence of N_2 also significantly influence NO_X emission levels. Increasing coal combustion temperature from 850 to 1300°C increased peak NO_X emissions by 50-70% for N_2-based inlet gas, and 30–50% for CO_2-based inlet gas [114]. Additionally, at combustion temperatures above 1300°C, thermal and prompt reaction pathways can occur, resulting in NO_X formation from N_2 in air [115, 106, 76]. Therefore, the higher AFT (well above 1300°C) that occurs as % biomass increases, enhances the influence of temperature on NO_X formation from N_2, thereby leading to increased NO_X emissions. In practice, combustion must be accurately controlled at specific conditions to achieve reductions in

NO_X emissions (*e.g.*, air staging, fuel staging) [106].

In many countries, there is increasing demand for improved power efficiency and emissions reduction of SO_X and NO_X due to stringent legislation [116]. Furthermore, the CO_2 capture process requires low levels of SO_X and NO_X in the flue gas to minimise amine solvent loss from the irreversible formation of heat stable salts [117]. For instance, MEA solvent requires SO_X flue gas concentration of 10 ppm to regulate solvent consumption (at ~1.6 kg of MEA per tonne CO_2 captured), whereas NO_X concentration should not exceed 20 ppmv [117, 118]. Thus, inherent reductions of SO_X and NO_X emissions by co-firing coal with biomass is extremely advantageous. Across the different co-firing scenarios, the flue gas NO_X concentration (between 118–149 ppb) was well below the NO_X tolerance limits of MEA. Co-firing medium sulphur coal with biomass resulted in SO_X concentrations between 0.2–7.1 ppm, which was also below amine requirements. Although co-firing high sulphur coal with 50% biomass could reduce SO_X concentrations by 43–80% to 420–1180 ppm compared to coal only combustion (2080 ppm), SO_X levels were still above the tolerance level of MEA. Hence, flue gas desulphurisation (FGD) would be required in all cases of high sulphur coal co-combustion. By selecting an appropriate combination of biomass and coal, it may be possible to satisfy both emission regulations and amine tolerance limits for SO_X and NO_X, without the need for additional pollution control technologies (*e.g.* FGD or selective catalytic reduction).

4.2. Heat recovery calculations

4.2.1. Recoverable heat

The results presented here are based on the co-combustion scenario of raw wheat straw (16% moisture) and high sulphur coal, where biomass co-firing proportion ranged between 0 to 50%. For scenarios that involved solvents with higher heat duty and reboiler temperature (*e.g.* MEA), heat recovery could not fulfil the energy requirements of solvent regeneration. The amount of recoverable heat was observed to increase with co-firing proportion, as increasing biomass share in the fuel blend resulted in a substantial increase of exhaust gas

temperature and flow rate. The range of recoverable heat results for different co-firing proportions and solvent scenarios are gathered in table 6. The minimum outlet temperature of the gas exiting the heat exchanger was found to be 113°C. This was well above the exhaust dew point of 40°C, thereby avoiding condensation in the exhaust and possible material damage (*e.g.* from condensed acids).

Table 6: Recoverable heat and area results for different solvent scenarios.

Solvent scenario	Recoverable heat (% heat duty)	Area (m^2)	Gas outlet temperature (°C)
MEA	53 – 100	6400 – 26000	138 – 271
Cansolv	84 – 100	2100 – 31400	138 – 412
"New solvent"	100	1500 – 8500	113 – 427

As figure 9 shows, at 50% co-firing, 100% of the heat duty in all three solvent scenarios could be supplied through the heat recovery system, clarifying the importance of heat recovery for BECCS efficiency enhancement.

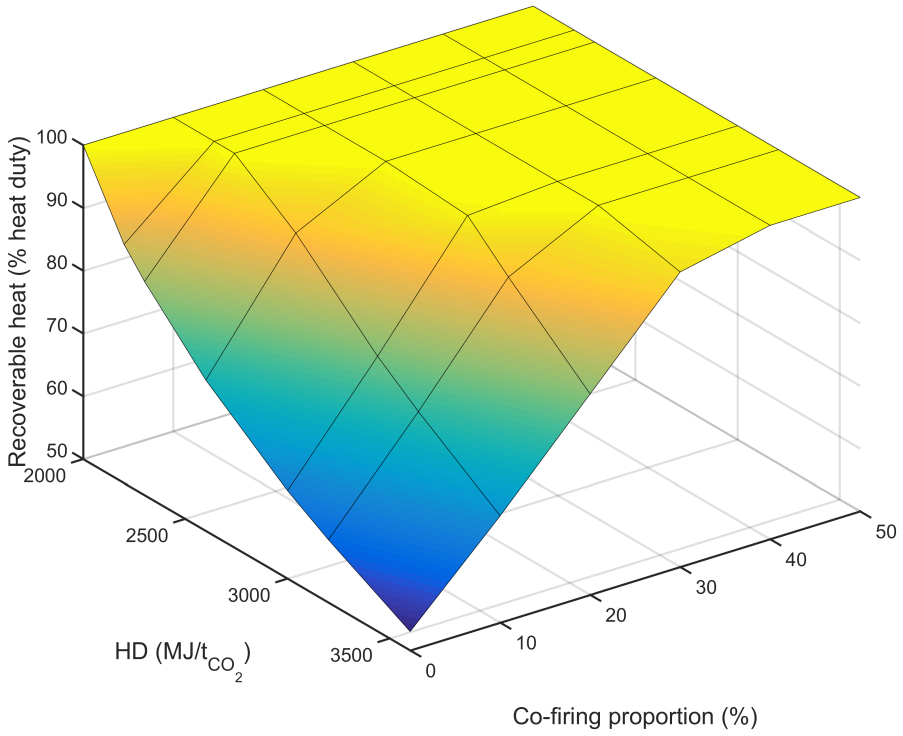

Figure 9: Recoverable heat (% reboiler heat duty) as a function of co-firing proportion (%) and solvent heat duty (MJ.t$^{-1}_{CO_2}$).

4.2.2. Efficiency and carbon intensity

The overall system efficiency increased as the performance of the post-combustion capture solvent improved (*e.g.* lower heat duty and reboiler temperature), shown in figure 10. With 100% heat recovery (HR), an efficiency (% HHV) of 38% was reached in the "new solvent" ("NS") case at 50% co-firing. Owing to their age, the current fleet of coal-fired power plants have efficiencies ranging from 26% (*e.g.* Australia or India) to 35% (*e.g.* Europe or US), with the world average of around 30% (LHV or slightly below 29% HHV) [119] . Thus, a 50% co-firing BECCS power plant could be 9% more efficient than the average coal-fired power plant in operation today.

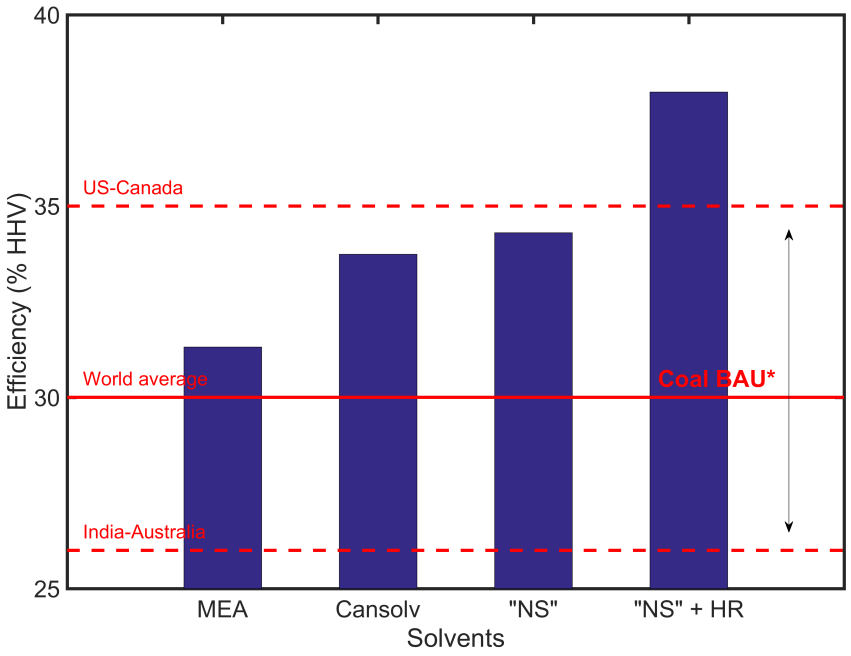

Figure 10: Plant efficiency (% HHV) for different solvent scenarios at 50% co-firing. NS = new solvent, HR = heat recovery, BAU = Business As Usual (average efficiencies around the world)

With improved system efficiency, less fuel is burned per MWh produced, *i.e.* less CO_2 is captured per MWh of electricity generated. As figure 11 demonstrates, carbon intensity decreases with lower system efficiency (*e.g.* higher heat duty solvent or increase co-firing %). Hence, the MEA system (31% HHV efficiency at 50% co-firing) captured -295 $kg_{CO_2}.MWh^{-1}$, whereas the "new solvent" system (34% HHV efficiency) captured -270 $kg_{CO_2}.MWh^{-1}$. At the same co-firing proportion of 50%, the "new solvent" system combined with 100% heat recovery—with higher efficiency of 38% HHV—captured only -245 $kg_{CO_2}.MWh^{-1}$.

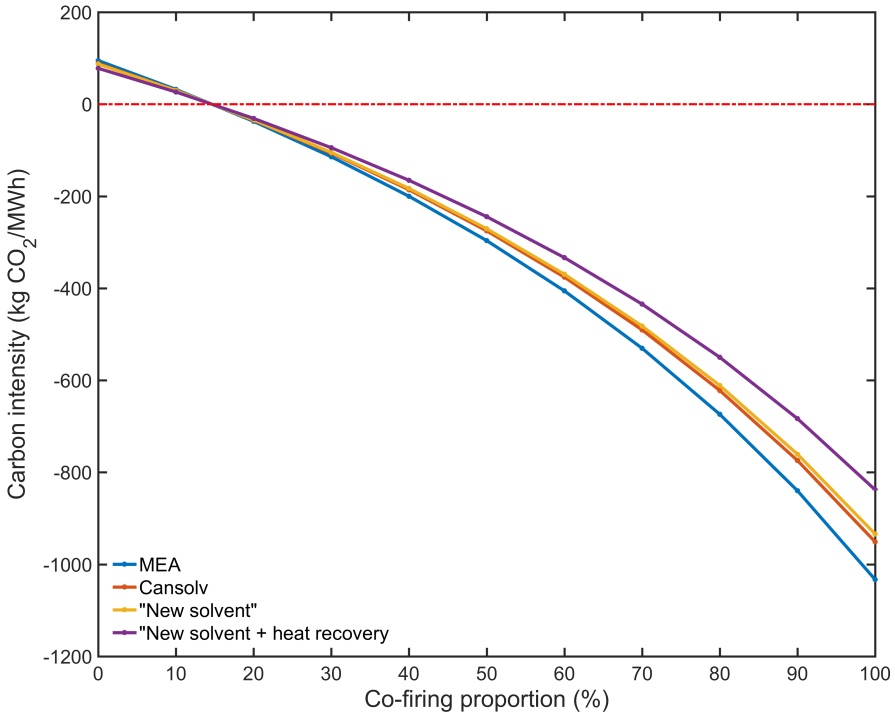

Figure 11: Plant carbon intensity as a function of co-firing for different solvent scenarios.

As a system with improved efficiency would be more economically competitive with other power generation systems, its annual dispatch factor would likely be higher than that of a less efficient system. Figure 12 shows the annual avoided carbon emissions as a function of efficiency and annual capacity (load factor %). An MEA capture system operating at 60% capacity would capture 0.66 Mt_{CO_2} per year. As illustrated on the figure, a more efficient system could capture the same amount of CO_2 on an annual basis if operating at a capacity factor of 72 %.

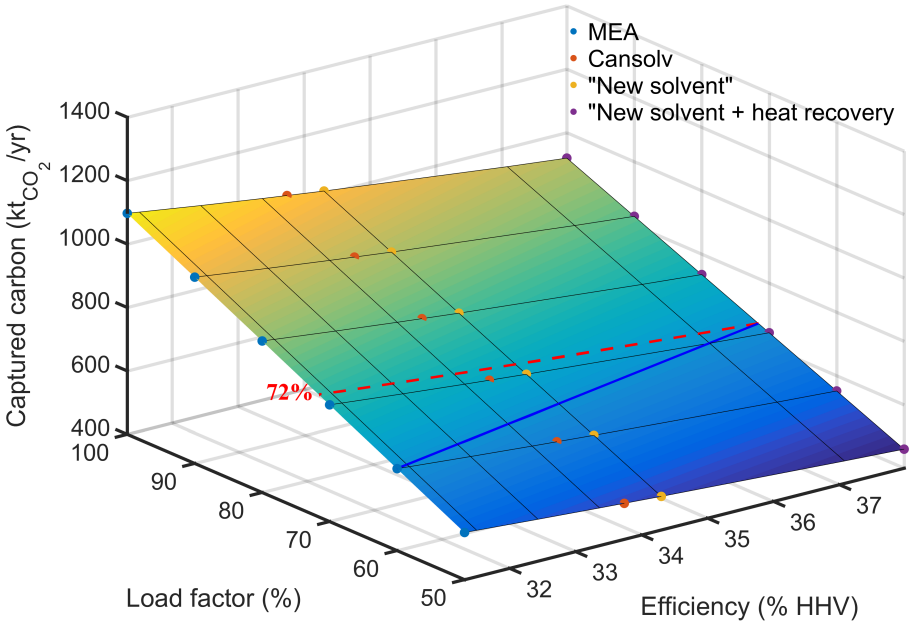

Figure 12: Annual negative carbon emissions ($Mt_{CO_2}.yr^{-1}$) as a function of system efficiency (% HHV) and capacity (%).

It is important to consider the complex trade-offs between carbon intensity and efficiency. On one hand, the low efficiency systems are preferable when it comes to achieving a higher mitigation target on a per MWh basis. However, the power generation efficiency is likely to impact the system's dispatch rate within an electricity market, hence potentially affecting its mitigation potential on a per year basis.

5. Conclusions

BECCS is a promising negative emissions technology, which has the potential to provide substantial reductions to CO_2 emissions. However, the CO_2 capture process and the use of biomass fuel both impose a significant efficiency penalty on the power plant. This study demonstrates that waste heat recovery from

the boiler system can provide significant improvements to BECCS power plant efficiency, while enabling large emissions reductions.

The equilibrium analysis of biomass co-combustion revealed that AFT was strongly influenced by moisture content and ash content. Blending coal with low moisture biomass significantly enhanced combustion performance. Compared to combustion of coal alone, 50% co-firing of biomass with 5 wt% moisture increased AFT by 136°C. In contrast, co-firing coal with biomass of 50% moisture only increased AFT by 4–5°C. High sulphur coal had lower ash content compared to medium sulphur coal, thus generated slightly higher AFT. The emissions of NO_X were much lower than SO_X, and well below the NO_X tolerance levels of amine solvents. Emissions of NO_X were strongly dependent on combustion conditions and increased with higher AFT. In practice however, combustion conditions are controlled to reduce NO_X emissions through air staging or fuel staging.

Another benefit of biomass co-firing is SO_X emission reduction, which could be attributed to decreased sulphur content and SO_X absorption by alkali oxides in ash. Although fuel sulphur content is a key factor, the analysis indicated that the metal oxides CaO, MgO, Na_2O, K_2O had a role in SO_X reduction. Other metal oxides (Al_2O_3, Fe_2O_3, MnO_2) not yet reported in literature were also involved in sulphur capture. Thus, further research is required on SO_X absorption by ash alkali oxides to understand the chemical mechanism and kinetics, particularly with respect to biomass co-firing applications. The co-firing of medium sulphur coal reduced flue gas SO_X concentration below tolerance limits of MEA solvent, which would eliminate the need for FGD, reducing the capital cost of this process and offsetting the added cost of heat recovery. This highlights the importance of appropriate fuel selection to meet the requirements for combustion performance and tolerance limits of the capture solvents.

The effect of waste heat recovery on BECCS system efficiency was investigated. Heat recovery from the boiler system could partially or completely supply heat duty for solvent regeneration as a function of fuel composition and solvent selection. At 0% biomass co-firing, heat recovery supplemented 50% of the heat

duty in the base solvent scenario. In contrast, recovered heat supplied 100% of the duty in the case of high performance solvent. Furthermore, heat recovery supplemented a greater fraction of heat duty as biomass co-firing increased, due to the increases in AFT and the exhaust gas flow rate. Subsequently, 100% of the solvent regeneration heat duty could thus be supplied through heat recovery at 50% co-firing for all solvent scenarios. Without the solvent heat duty penalty, the efficiency penalty of a 50% co-firing power plant with post-combustion capture drops from 11.6 % (conventional MEA system) to 4.9 % (using 100% heat recovery). Such a system could reach a 38% efficiency, which is 9% more efficient than the currently installed coal-fired power plant fleet. Thus, this approach has the potential to significantly reduce the limitations of co-firing biomass in power plants.

The study of power plant carbon capture potential indicated that an increase in the system efficiency resulted in the decrease of plant carbon negativity. High efficiency power plants burn less fuel per MWh of electricity produced, hence less CO_2 is captured. At 50% co-firing, a low efficiency system using MEA solvent with no heat recovery captures 50 tons more of the CO_2 than a high efficiency system with heat recovery. In a 2050 future, where the main objective would be to drastically curb carbon emissions, low efficiency BECCS, which captures more CO_2, could possibly be preferable over high efficiency systems. However, these plants would have a substantially greater marginal cost of electricity generation, and would therefore likely be economically viable only in the event that a payment is available for removing CO_2 from the atmosphere. This highlights the importance of the metric chosen - power generation efficiency or carbon intensity - in the evaluation of BECCS performance.

6. Acknowledgements

The authors would like to acknowledge funding from the EPSRC under grants EP/M001369/1 (MESMERISE-CCS), EP/M015351/1 (Opening New Fuels for UK Generation) and EP/N024567/1 (CCSInSupply). Mathilde Fajardy thanks

Imperial College London for funding a PhD scholarship.

Appendix A. Appendix

Appendix A.1. Comparison of fuel properties

Table A1: Typical fuel properties of coal, wood biomass and herbaceous biomass (*e.g.* straw, grass), adapted from Veijonen *et al.* (2003) [120].

Property	Coal	Wood	Herbaceous biomass
Ash content (wt% dry)	8.5–10.9	0.4–4.0	5–7.5
Moisture content (wt% wet)	6–10	5–60	15–25
Lower heating value, LHV (MJ/kg)	26.0–28.3	18.4–20.0	17.1–17.5
C (wt% dry)	76–87	47–52	45–47
H (wt% dry)	3.5–5.5	5.8–6.7	5.7–6.0
O (wt% dry)	2.8–11.3	38–46	40–46
Cl (wt% dry)	<0.1	0.01–0.05	0.09–0.97
S (wt% dry)	0.5–3.1	0.02–0.10	0.05–0.2
N (wt% dry)	0.8–1.5	0.1–0.8	0.4–1.04

Appendix A.2. Ash composition of the coal and biomass

Table A2: Coal and biomass ash composition used for modelling in FactSage.

Composition	High sulphur coal	Medium sulphur coal	Clean wood chips	Wheat straw
SiO_2 (% ash)	46.8	50	43.1	56.2
Al_2O_3 (% ash)	18.0	30.0	8.9	1.2
Fe_2O_3 (% ash)	20.0	9.8	3.9	1.2
CaO (% ash)	7.0	4.0	28.0	6.5
MgO (% ash)	1.0	0.5	4.2	3.0
Na_2O (% ash)	0.6	0.1	2.0	1.3
K_2O (% ash)	1.9	0.1	5.5	23.7
TiO_2 (% ash)	1.0	2.0	0.4	0.06
P_2O_5 (% ash)	0.2	1.8	2.2	4.4
SO_3 (% ash)	3.5	1.7	1.8	1.1
MnO_2 (% ash)	0	0	0	1.34
References	[58]	[59]	[59]	[61, 121]

Appendix A.3. Adiabatic flame temperature (AFT) results

Table A3: AFT for various biomass and coal co-firing scenarios at different biomass % and $\lambda = 1.3$. Refer to table 4 for fuel types in each scenario. Final row shows the temperature difference between AFT at 50% biomass co-firing and 0% co-firing.

AFT (°C) for different coal and biomass blending scenarios								
Biomass %	A	B	C	D	E	F	G	H
0	2181.63	2181.63	2181.63	2181.63	2189.58	2189.58	2189.58	2189.58
5	2194.68	2191.68	2194.40	2182.01	2202.34	2199.20	2202.30	2189.76
10	2207.58	2201.77	2207.03	2182.41	2215.76	2209.64	2215.61	2189.96
15	2220.32	2211.87	2219.51	2182.84	2228.91	2220.10	2228.63	2190.17
20	2232.88	2221.98	2231.82	2183.31	2242.09	2230.34	2242.38	2190.56
25	2245.62	2232.10	2245.43	2183.81	2255.78	2241.02	2256.13	2191.07
30	2259.47	2242.37	2259.81	2184.34	2269.46	2252.12	2269.87	2191.60
35	2273.74	2253.88	2274.40	2184.91	2283.12	2263.34	2283.63	2192.14
40	2288.25	2265.50	2288.97	2185.52	2296.81	2274.68	2297.11	2192.71
45	2302.76	2277.78	2303.51	2186.18	2310.50	2286.15	2309.80	2193.10
50	2317.25	2290.19	2318.00	2186.89	2323.97	2297.71	2322.22	2193.49
T(50%) - T(0%)	135.62	108.56	136.37	5.26	134.39	108.13	132.64	3.91

References

[1] C. Marchetti, On geoengineering and the CO_2 problem, Climatic Change 1 (1) (1977) 59–68.

[2] IPCC, Climate Change 2014: Mitigation of Climate Change. Working Group III Contribution to the Fifth Assessment Report of the Intergovernmental Panel on Climate Change., Cambridge University Press, Cambridge, United Kingdom and New York, NY, USA, 2014.

[3] COP21, The 2015 United Nations Climate Change Conference, 30 November to 12 December 2015, http://www.cop21.gouv.fr/en/.

[4] R. H. Williams, Fuel Decarbonization for Fuel Cell Applications and Sequestration of the Separated CO_2 CEES Report 295, Tech. rep., Center for Energy and Environmental Studies, Princeton University (1996).

[5] H. J. Herzog, E. M. Drake, Carbon dioxide recovery and disposal from large energy systems, Annual Review of Energy and the Environment 21 (1996) 145–166.

[6] L. Gustavsson, P. Börjesson, B. Johansson, P. Svenningsson, Reducing CO_2 emissions by substituting biomass for fossil fuels, Energy 20 (11) (1995) 1097–1113.

[7] L. Gustavsson, P. Svenningsson, Substituting fossil fuels with biomass, Energy Conversion and Management 37 (6–8) (1996) 1211–1216.

[8] F. Kraxner, S. Nilsson, M. Obersteiner, Negative emissions from BioEnergy use, carbon capture and sequestration (BECS)–the case of biomass production by sustainable forest management from semi-natural temperate forests, Biomass and Bioenergy 24 (4–5) (2003) 285–296.

[9] S. Fuss, J. G. Canadell, G. P. Peters, M. Tavoni, R. M. Andrew, P. Ciais, R. B. Jackson, C. D. Jones, F. Kraxner, N. Nakicenovic, C. Le Quere, M. R. Raupach, A. Sharifi, P. Smith, Y. Yamagata, Betting on negative emissions, Nature Climate Change 4 (10) (2014) 850–853.

[10] C. Azar, K. Lindgren, M. Obersteiner, K. Riahi, D. P. van Vuuren, K. M. G. J. den Elzen, K. Möllersten, E. D. Larson, The feasibility of low CO_2 concentration targets and the role of bio-energy with carbon capture and storage (BECCS), Climatic Change 100 (1) (2010) 195–202.

[11] C. Gough, P. Upham, Biomass energy with carbon capture and storage (BECCS): a review, Working Paper 147, Report, Tyndall Centre for Climate Change Research, University of Manchester (2010).

[12] M. C. Carbo, R. Smit, B. van der Drift, D. Jansen, Bio energy with CCS (BECCS): Large potential for BioSNG at low CO_2 avoidance cost, in: 10th International Conference on Greenhouse Gas Control Technologies, September 2010, Amsterdam, The Netherlands, Vol. 4, Energy Procedia, 2011, pp. 2950–2954.

[13] F. Kraxner, G. Kindermann, S. Leduc, K. Aoki, M. Obersteiner, Bioenergy use for negative emissions - potentials for carbon capture and storage (BECCS) from a global forest model combined with optimized siting and scaling of bioenergy plants in Europe, in: First International Workshop on Biomass & Carbon Capture and Storage, October 2010, University of Orléans, France, 2010.

[14] W. Schakel, H. Meerman, A. Talaei, A. Ramirez, A. Faaij, Comparative life cycle assessment of biomass co-firing plants with carbon capture and storage, Applied Energy 131 (2014) 441–467.

[15] K. Al-qayim, W. Nimmo, M. Pourkashanian, Comparative techno-economic assessment of biomass and coal with CCS technologies in a pulverized combustion power plant in the United Kingdom, International Journal of Greenhouse Gas Control 43 (2015) 82–92.

[16] J. R. Moreira, V. Romeiro, S. Fuss, F. Kraxner, S. A. Pacca, BECCS potential in Brazil: Achieving negative emissions in ethanol and electricity production based on sugar cane bagasse and other residues, Applied Energy 179 (2016) 55–63.

[17] F. Kraxner, K. Aoki, S. Leduc, G. Kindermann, S. Fuss, J. Yang, Y. Yamagata, K. I. Tak, M. Obersteiner, BECCS in South Korea-Analyzing the negative emissions potential of bioenergy as a mitigation tool, Renewable Energy 61 (2014) 102–108.

[18] J. S. Rhodes, D. W. Keith, Engineering economic analysis of biomass IGCC with carbon capture and storage, Biomass and Bioenergy 29 (6) (2005) 440–450.

[19] K. Möllersten, J. Yan, J. R. Moreira, Potential market niches for biomass energy with CO_2 capture and storage – Opportunities for energy supply with negative CO_2 emissions, Biomass and Bioenergy 25 (3) (2003) 273–285.

[20] K. Möllersten, L. Gao, J. Yan, M. Obersteiner, Efficient energy systems with CO_2 capture and storage from renewable biomass in pulp and paper mills, Renewable Energy 29 (9) (2004) 1583–1598.

[21] D. Loeffler, N. Anderson, Emissions tradeoffs associated with cofiring forest biomass with coal: A case study in Colorado, USA, Applied Energy 113 (2014) 67–77.

[22] K. Savolainen, Co-firing of biomass in coal-fired utility boilers, Applied Energy 74 (3–4) (2003) 369–381.

[23] Drax, Annual report and accounts 2014: Power in perspective, Report, Drax Group plc, Drax Power Station, North Yorkshire, UK (2014).

[24] K. Fletcher, Drax's 2014 results show decarbonization project on time, budget, no. 17/1/2017, Wood Pellet Services, 2015.
URL http://www.woodpelletservices.com/documents/Drax%20FEB2015.pdf

[25] IEA, IEA Energy Technology Essentials: Biomass for Power Generation and CHP, Tech. Rep. 17/1/2017 (2007).
URL http://www.iea.org/publications/freepublications/publication/essentials3.pdf

[26] Z. Liu, T. G. Johnson, I. Altman, The moderating role of biomass availability in biopower co-firing—A sensitivity analysis, Journal of Cleaner Production 135 (2016) 523–532.

[27] S. Evans, Investigation: Does the UK's biomass burning help solve climate change?, no. 17/1/2017, CarbonBrief, 2015.
URL https://www.carbonbrief.org/investigation-does-the-uks-biomass-burning-help-solve-

[28] L. L. Sloss, Emission from cofiring coal, biomass and sewage sludge, CCC/175, IEA Clean Coal Centre, London, United Kingdom, 2010.

[29] K. Goto, K. Yogo, T. Higashii, A review of efficiency penalty in a coal-fired power plant with post-combustion CO_2 capture, Applied Energy 111 (2013) 710–720.

[30] A. Austin, Size Matters, no. 17/1/17, Biomass Magazine, BBI International, http://biomassmagazine.com/articles/2309/size-matters, 2017.

[31] G. Kosmadakis, S. Karellas, E. Kakaras, Renewable and conventional electricity generation systems: Technologies and diversity of energy systems, Springer London, London, 2013, pp. 9–30.

[32] N. Mac Dowell, N. Shah, The multi-period optimisation of an amine-based CO_2 capture process integrated with a super-critical coal-fired power station for flexible operation, Computers & Chemical Engineering 74 (2015) 169–183.

[33] N. Mac Dowell, I. Staffell, The role of flexible CCS in the UK's future energy system, International Journal of Greenhouse Gas Control 48, Part 2 (Flexible operation of carbon capture plants) (2016) 327–344.

[34] IEAGHG, Potential for biomass and carbon dioxide capture and storage, Report 2011/06, IEA Greenhouse Gas R&D Programme (IEA GHG), Cheltenham, United Kingdom, 2011.

[35] J. Oexmann, A. Kather, Minimising the regeneration heat duty of post-combustion CO_2 capture by wet chemical absorption: The misguided focus on low heat of absorption solvents, International Journal of Greenhouse Gas Control 4 (1) (2010) 36–43.

[36] L. M. Romeo, S. Espatolero, I. Bolea, Designing a supercritical steam cycle to integrate the energy requirements of CO_2 amine scrubbing, International Journal of Greenhouse Gas Control 2 (4) (2008) 563–570.

[37] M. Lucquiaud, J. Gibbins, On the integration of CO_2 capture with coal-fired power plants: A methodology to assess and optimise solvent-based

699 post-combustion capture systems, Chemical Engineering Research and
700 Design 89 (9) (2011) 1553–1571.

701 [38] E. Sanchez Fernandez, M. Sanchez del Rio, H. Chalmers, P. Khakharia,
702 E. L. V. Goetheer, J. Gibbins, M. Lucquiaud, Operational flexibility op-
703 tions in power plants with integrated post-combustion capture, Interna-
704 tional Journal of Greenhouse Gas Control 48, Part 2 (Flexible operation
705 of carbon capture plants) (2016) 275–289.

706 [39] N. Y. Nsakala, J. Marion, C. Bozzuto, G. Liljedahl, M. Palkes, D. Vogel,
707 M. Guha, H. Johnson, S. Plasynski, Engineering feasibility of CO_2 capture
708 on an existing US coal-fired power plant, in: First National Conference
709 on Carbon Sequestration, U.S. Department of Energy (DOE), National
710 Energy Technology Laboratory, 2001.

711 [40] M. Lucquiaud, J. Gibbins, Effective retrofitting of post-combustion CO_2
712 capture to coal-fired power plants and insensitivity of CO_2 abatement
713 costs to base plant efficiency, International Journal of Greenhouse Gas
714 Control 5 (3) (2011) 427–438.

715 [41] N. Ceccarelli, M. van Leeuwen, T. Wolf, P. van Leeuwen, R. van der Vaart,
716 W. Maas, A. Ramos, Flexibility of low-CO_2 gas power plants: Integration
717 of the CO_2 capture unit with CCGT operation, in: 12th International
718 Conference on Greenhouse Gas Control Technologies (GHGT-12), Vol. 63,
719 Energy Procedia, pp. 1703–1726.

720 [42] M. Thern, K. Jordal, M. Genrup, Temporary CO_2 capture shut down:
721 Implications on low pressure steam turbine design and efficiency, in: 7th
722 Trondheim Conference on CO_2 capture, Transport and Storage, Vol. 51,
723 Energy Procedia, 2014, pp. 14–23.

724 [43] M. Lucquiaud, E. S. Fernandez, H. Chalmers, N. M. Dowell, J. Gibbins,
725 Enhanced operating flexibility and optimised off-design operation of coal
726 plants with post-combustion capture, in: 12th International Conference

on Greenhouse Gas Control Technologies (GHGT-12), Vol. 63, Energy Procedia, 2014, pp. 7494–7507.

[44] M. Lucquiaud, J. Gibbins, Steam cycle options for the retrofit of coal and gas power plants with postcombustion capture, in: 10th International Conference on Greenhouse Gas Control Technologies (GHGT-10), Vol. 4, Energy Procedia, 2011, pp. 1812–1819.

[45] T. Sanpasertparnich, R. Idem, I. Bolea, D. deMontigny, P. Tontiwachwuthikul, Integration of post-combustion capture and storage into a pulverized coal-fired power plant, International Journal of Greenhouse Gas Control 4 (3) (2010) 499–510.

[46] I. Pfaff, J. Oexmann, A. Kather, Optimised integration of post-combustion CO_2 capture process in greenfield power plants, Energy 35 (10) (2010) 4030–4041.

[47] IEAGHG, CO_2 capture in low rank coal power plants, Technical Study 2006/1, IEA Greenhouse Gas R&D Programme (IEA GHG), Cheltenham, United Kingdom, 2006.

[48] C. Wang, B. He, S. Sun, Y. Wu, N. Yan, L. Yan, X. Pei, Application of a low pressure economizer for waste heat recovery from the exhaust flue gas in a 600 MW power plant, Energy 48 (1) (2012) 196–202.

[49] X. Wang, Z. Hu, S. Deng, Y. Xiong, H. Tan, Effect of biomass/coal cofiring and air staging on NO_X emission and combustion efficiency in a drop tube furnace, in: J. Yan, D. J. Lee, S. K. Chou, U. Desideri, H. Li (Eds.), International Conference on Applied Energy (ICAE2014), Vol. 61, Energy Procedia, 2014, pp. 2331–2334.

[50] G. Xu, S. Huang, Y. Yang, Y. Wu, K. Zhang, C. Xu, Techno-economic analysis and optimization of the heat recovery of utility boiler flue gas, Applied Energy 112 (2013) 907–917.

[51] G. Xu, C. Xu, Y. Yang, Y. Fang, Y. Li, X. Song, A novel flue gas waste heat recovery system for coal-fired ultra-supercritical power plants, Applied Thermal Engineering 67 (1–2) (2014) 240–249.

[52] T. Harkin, A. Hoadley, B. Hooper, Process integration analysis of a brown coal-fired power station with CO_2 capture and storage and lignite drying, Energy Procedia 1 (1) (2009) 3817–3825.

[53] T. Harkin, A. Hoadley, B. Hooper, Reducing the energy penalty of CO_2 capture and compression using pinch analysis, Journal of Cleaner Production 18 (9) (2010) 857–866.

[54] S. Basu, A. K. Debnath, Chapter IV General Instruments: Temperature Measurement - Various Measuring Points and Range Selection, Academic Press (imprint of Elsevier Ltd.), London, UK, 2015, pp. Pages 241–244.

[55] Mac Dowell, Niall and Fajardy, Mathilde, On the potential for BECCS efficiency improvement through heat recovery from both post-combustion and oxy-combustion facilities, Faraday Discussions 192 (0) (2016) 241–250.

[56] P. Quaak, H. Knoef, H. E. Stassen, Energy from Biomass: A review of Combustion and Gasification Technologies, World bank Technical Paper No. 422 Energy Series, The International Bank for Reconstruction and Development, Washington, United States, 1999.

[57] L. Westerlund, R. Hermansson, J. Fagerström, Flue gas purification and heat recovery: A biomass fired boiler supplied with an open absorption system, Applied Energy 96 (2012) 444–450.

[58] M. B. Berkenpas, J. J. Fry, K. Kietzke, E. S. Rubin, Integrated Environmental Control Model Getting Started, Tech. Rep. April, Center for Energy and Environmental Studies, Carnegie Mellon University (2001).

[59] IEAGHG, CO_2 Capture at Coal Based Power and Hydrogen Plants, Report, International Energy Agency Greenhouse Gas R&D Programme (IEAGHG) (2014).

[60] R. Parajuli, M. T. Knudsen, J. H. Schmidt, T. Dalgaard, Life Cycle Assessment of district heat production in a straw fired CHP plant, Biomass and Bioenergy 68 (September) (2014) 115–134.

[61] H. Spliethoff, K. R. G. Hein, Effect of co-combustion of biomass on emissions in pulverized fuel furnaces, Fuel Processing Technology 54 (1–3) (1998) 189–205.

[62] T. Heinzel, V. Siegle, H. Spliethoff, K. R. G. Hein, Investigation of slagging in pulverized fuel co-combustion of biomass and coal at a pilot-scale test facility, Fuel Processing Technology 54 (1998) 109–125.

[63] ISO, Solid biofuels – Fuel specifications and classes. Part 1: General requirements, Tech. rep. (2014).

[64] M. Campbell, Technology innovation & advancements for Shell Cansolv CO_2 capture solvents, in: 12th International Conference on Greenhouse Gas Control Technologies (GHGT-12), Vol. 63, Energy Procedia, pp. 801–807.

[65] A. Singh, K. Stéphenne, Shell Cansolv CO_2 capture technology: Achievement from First Commercial Plant, in: 12th International Conference on Greenhouse Gas Control Technologies (GHGT-12), Vol. 63, Energy Procedia, pp. 1678–1685.

[66] Q. Ye, X. Wang, Y. Lu, Screening and evaluation of novel biphasic solvents for energy-efficient post-combustion CO_2 capture, International Journal of Greenhouse Gas Control 39 (2015) 205–214.

[67] L. V. van der Ham, E. L. V. Goetheer, E. S. Fernandez, M. R. M. Abu-Zahra, T. J. H. Vlugt, Precipitating amino acid solutions, Woodhead Publishing, Cambridge, 2016, pp. 103–119.

[68] S. Wang, Z. Xu, Dual-liquid phase systems, Woodhead Publishing, Cambridge, 2016, pp. 201–223.

[69] G. Rochelle, E. Chen, S. Freeman, D. Van Wagener, Q. Xu, A. Voice, Aqueous piperazine as the new standard for CO_2 capture technology, Chemical Engineering Journal 171 (3) (2011) 725–733.

[70] L. Raynal, P. Alix, P.-A. Bouillon, A. Gomez, M. l. F. de Nailly, M. Jacquin, J. Kittel, A. di Lella, P. Mougin, J. Trapy, The DMX^{TM} process: An original solution for lowering the cost of post-combustion carbon capture, Energy Procedia 4 (2011) 779–786.

[71] P. Markewitz, W. Kuckshinrichs, W. Leitner, J. Linssen, P. Zapp, R. Bongartz, A. Schreiber, T. E. Muller, Worldwide innovations in the development of carbon capture technologies and the utilization of CO_2, Energy & Environmental Science 5 (6) (2012) 7281–7305.

[72] Y. Zhang, B. Freeman, P. Hao, G. T. Rochelle, Absorber modeling for ngcc carbon capture with aqueous piperazine, Faraday Discussions 192 (0) (2016) 459–477.

[73] C. W. Bale, P. Chartrand, S. A. Degterov, G. Eriksson, K. Hack, R. Ben Mahfoud, J. Melançon, A. D. Pelton, S. Petersen, FactSage thermochemical software and databases, Calphad 26 (2) (2002) 189–228.

[74] C. W. Bale, E. Bélisle, P. Chartrand, S. A. Decterov, G. Eriksson, K. Hack, I. H. Jung, Y. B. Kang, J. Melançon, A. D. Pelton, C. Robelin, S. Petersen, FactSage thermochemical software and databases – recent developments, Calphad 33 (2) (2009) 295–311.

[75] M. Blander, T. A. Milne, D. C. Dayton, R. Backman, D. Blake, V. Kühnel, W. Linak, A. Nordin, A. Ljung, Equilibrium chemistry of biomass combustion: A round-robin set of calculations using available computer programs and databases, Energy & Fuels 15 (2) (2001) 344–349.

[76] I. Obernberger, T. Brunner, G. Bärnthaler, Chemical properties of solid biofuels–significance and impact, Biomass and Bioenergy 30 (11) (2006) 973–982.

[77] A. George, M. Larrion, D. Dugwell, P. S. Fennell, R. Kandiyoti, Co-firing of single, binary, and ternary fuel blends: Comparing synergies within trace element partitioning arrived at by thermodynamic equilibrium modeling and experimental measurements, Energy & Fuels 24 (5) (2010) 2918–2923.

[78] X. Wei, U. Schnell, K. R. G. Hein, Behaviour of gaseous chlorine and alkali metals during biomass thermal utilisation, Fuel 84 (7–8) (2005) 841–848.

[79] W. L. Luyben, Heat exchanger simulations involving phase changes, Computers and Chemical Engineering 67 (2014) 133–136.

[80] Thermopedia, http://thermopedia.com/content/1150Begal, 2016.

[81] Spiraxsarco, http://www.spiraxsarco.com/Resources/Pages/steam-tables.aspx, 2016.

[82] R. Sinnott, G. Towler, Heat-Transfer Equipment, Chemical Engineering Design (2008) 815–978.

[83] R. H. Perry, D. W. Green, Perry's Chemical Engineers' Handbook, 15th Edition, The McGraw-Hill Companies, Inc., New York, US, 2008.

[84] R. C. Flagan, J. H. Seinfeld, Chapter 2 Combustion Fundamentals, Dover Publications Inc., New York, United States, 2012.

[85] B. M. Jenkins, L. L. Baxter, T. R. Miles Jr, T. R. Miles, Combustion properties of biomass, Fuel Processing Technology 54 (1–3) (1998) 17–46.

[86] M. Sami, K. Annamalai, M. Wooldridge, Co-firing of coal and biomass fuel blends, Progress in Energy and Combustion Science 27 (2) (2001) 171–214.

[87] W. L. Van De Kamp, D. J. Morgan, The co-firing of pulverised bituminous coals with straw, waste paper and municipal sewage sludge, Combustion Science and Technology 121 (1–6) (1996) 317–332.

[88] H. Spliethoff, W. Scheurer, K. R. G. Hein, Effect of co-combustion of sewage sludge and biomass on emissions and heavy metals behaviour, Process Safety and Environmental Protection 78 (1) (2000) 33–39.

[89] A. Demirbaş, Combustion characteristics of different biomass fuels, Progress in Energy and Combustion Science 30 (2) (2004) 219–230.

[90] A. Demirbaş, Potential applications of renewable energy sources, biomass combustion problems in boiler power systems and combustion related environmental issues, Progress in Energy and Combustion Science 31 (2) (2005) 171–192.

[91] L. Cheng, X. P. Ye, B. C. English, D. Boylan, T. Johnson, B. Zemo, Co-firing switchgrass in a 60-megawatt pulverized coal-fired boiler: Effects on combustion behavior and pollutant emissions, Energy Sources, Part A: Recovery, Utilization, and Environmental Effects 38 (3) (2016) 322–329.

[92] D. Fleig, K. Andersson, F. Johnsson, B. Leckner, Conversion of sulfur during pulverized oxy-coal combustion, Energy & Fuels 25 (2) (2011) 647–655.

[93] M. Müller, U. Schnell, G. Scheffknecht, Modelling the fate of sulphur during pulverized coal combustion under conventional and oxy-fuel conditions, in: 11th International Conference on Greenhouse Gas Control Technologies (GHGT-11), Vol. 37, Energy Procedia, 2013, pp. 1377–1388.

[94] R. K. Srivastava, C. A. Miller, C. Erickson, R. Jambhekar, Emissions of sulfur trioxide from coal-fired power plants, Journal of the Air & Waste Management Association 54 (6) (2004) 750–762.

[95] P. Marier, H. P. Dibbs, The catalytic conversion of SO_2 to SO_3 by fly ash and the capture of SO_2 and SO_3 by CaO and MgO, Thermochimica Acta 8 (1) (1974) 155–165.

[96] L. P. Belo, L. K. Elliott, R. J. Stanger, R. Spörl, K. V. Shah, J. Maier, T. F. Wall, High-temperature conversion of SO_2 to SO_3: Homogeneous experiments and catalytic effect of fly ash from air and oxy-fuel firing, Energy & Fuels 28 (11) (2014) 7243–7251.

[97] K. A. Graham, A. F. Sarofim, Inorganic aerosols and their role in catalyzing sulfuric acid production in furnaces, Journal of the Air & Waste Management Association 48 (2) (1998) 106–112.

[98] S. Li, T. Xu, P. Sun, Q. Zhou, H. Tan, S. Hui, NO_X and SO_X emissions of a high sulfur self-retention coal during air-staged combustion, Fuel 87 (6) (2008) 723–731.

[99] V. R. Gray, Retention of sulphur by laboratory-prepared ash from low-rank coal, Fuel 65 (11) (1986) 1618–1619.

[100] J. V. Ibarra, J. M. Palacios, A. M. de Andrés, Analysis of coal and char ashes and their ability for sulphur retention, Fuel 68 (7) (1989) 861–867.

[101] A. B. Fuertes, V. Artos, J. J. Pis, G. Marbán, J. M. Palacios, Sulphur retention by ash during fluidized bed combustion of bituminous coals, Fuel 71 (5) (1992) 507–511.

[102] C. Sheng, M. Xu, J. Zhang, Y. Xu, Comparison of sulphur retention by coal ash in different types of combustors, Fuel Processing Technology 64 (1–3) (2000) 1–11.

[103] K. V. Narayanan, E. Natarajan, Experimental studies on cofiring of coal and biomass blends in India, Renewable Energy 32 (15) (2007) 2548–2558.

[104] M. M. Roy, K. W. Corscadden, An experimental study of combustion and emissions of biomass briquettes in a domestic wood stove, Applied Energy 99 (2012) 206–212.

[105] M. M. Roy, A. Dutta, K. Corscadden, An experimental study of combustion and emissions of biomass pellets in a prototype pellet furnace, Applied Energy 108 (2013) 298–307.

[106] T. Nussbaumer, Combustion and co-combustion of biomass: Fundamentals, technologies, and primary measures for emission reduction, Energy & Fuels 17 (6) (2003) 1510–1521.

[107] A. Gani, K. Morishita, K. Nishikawa, I. Naruse, Characteristics of co-combustion of low-rank coal with biomass, Energy & Fuels 19 (4) (2005) 1652–1659.

[108] X. Wei, X. Guo, S. Li, X. Han, U. Schnell, G. Scheffknecht, B. Risio, Detailed modeling of NO_X and SO_X formation in co-combustion of coal and biomass with reduced kinetics, Energy & Fuels 26 (6) (2012) 3117–3124.

[109] R. Yoshiie, N. Hikosaka, Y. Nunome, Y. Ueki, I. Naruse, Effects of flue gas re-circulation and nitrogen contents in coal on NO_X emissions under oxy-fuel coal combustion, Fuel Processing Technology 136 (2015) 106–111.

[110] D. W. Pershing, J. O. L. Wendt, Relative contributions of volatile nitrogen and char nitrogen to NO_X emissions from pulverized coal flames, Industrial & Engineering Chemistry Process Design and Development 18 (1) (1979) 60–67.

[111] S. Kambara, T. Takarada, M. Toyoshima, K. Kato, Relation between functional forms of coal nitrogen and NO_X emissions from pulverized coal combustion, Fuel 74 (9) (1995) 1247–1253.

[112] M. A. Wójtowicz, J. R. Pels, J. A. Moulijn, The fate of nitrogen functionalities in coal during pyrolysis and combustion, Fuel 74 (4) (1995) 507–516.

[113] H. Spliethoff, U. Greul, H. Rüdiger, K. R. G. Hein, Basic effects on NO_X emissions in air staging and reburning at a bench-scale test facility, Fuel 75 (5) (1996) 560–564.

[114] Y. Hu, S. Naito, N. Kobayashi, M. Hasatani, CO_2, NO_X and SO_2 emissions from the combustion of coal with high oxygen concentration gases, Fuel 79 (15) (2000) 1925–1932.

[115] EPA, Technical bulletin: Nitrogen oxides (NO_X), why and how they are controlled, Tech. rep., North Carolina, US (1999).

[116] I. Barnes, Understanding pulverized coal, biomass and waste combustion, CCC/205, IEA Clean Coal Centre, London, United Kingdom, 2012.

[117] D. Adams, Flue gas treatment for CO_2 capture, CCC/169, IEA Clean Coal Centre, London, United Kingdom, 2010.

[118] M. Azzi, S. Day, D. French, B. Halliburton, A. Element, O. Farrell, P. Feron, Impact of flue gas impurities on amine-based PCC plants – Final Report, Australian National Low Emissions Coal Research and Development (ANLEC R&D), CSIRO, Australia, 2013.

[119] IEA, OECD, Power Generation from Coal: Measuring and Reporting Efficiency Performance and CO_2 Emissions, Tech. rep. (2010).

[120] K. Veijonen, P. Vainikka, T. Järvinen, E. Alakangas, Biomass co-firing - an efficient way to reduce greenhouse gas emissions, Report, European Bioenergy Networks (EUBIONET), VTT Processes (2003).

[121] S. V. Vassilev, D. Baxter, L. K. Andersen, C. G. Vassileva, An overview of the chemical composition of biomass, Fuel 89 (5) (2010) 913–933.